Advances in Science and Technology Research Journal

Advances in Science and Technology Research Journal, 2026, 20(4), 291–306
https://doi.org/10.12913/22998624/214994
ISSN 2299-8624, License CC-BY 4.0

Received: 2025.09.21
Accepted: 2026.02.15
Published: 2026.03.01

Improving the durability and wear performance of heat-polymerized poly(methyl methacrylate) using nanoparticles derived from hydroxyapatite and date seeds for denture base application

Howida Mohamed[1*], W. Y. Ali[2], Abdallah Shokry[1], A. H. Badran[2], Ameer Ali Kamel[2]

[1] Department of Mechanical Engineering, Faculty of Engineering, Fayoum University, Fayoum 63514, Egypt
[2] Department of Production Engineering and Mechanical Design, Faculty of Engineering, Minia University, Minia 61111, Egypt
* Corresponding author's e-mail: hma17@fayoum.edu.eg

ABSTRACT

This study aimed to develop and characterize a heat- polymerized poly(methyl methacrylate) (PMMA) denture base nanocomposite reinforced with hydroxyapatite nanoparticles (HA NPs) and economically synthesized date seed nanoparticles (DS NPs) to enhance its mechanical and tribological properties. Nanocomposites were fabricated with varying concentrations (0, 0.2, 0.4, 0.6, 0.8, and 1.0 wt.%) of HA NPs and DS NPs. The mechanical performance was evaluated through compression testing and Shore D hardness measurements. Tribological properties were assessed using a pin-on-disk tribometer against emery paper, stainless steel and PMMA counterfaces, measuring weight loss, wear rate (Wr), and the coefficient of friction (COF). X-ray diffraction (XRD) was used to characterize the crystallographic structure and structural properties of nanocomposite. Differential scanning calorimetry (DSC) for characterizing the thermal behavior and stability of materials. Morphological analysis of wear tracks was conducted via scanning electron microscopy (SEM). The morphological features and aggregation behavior of the synthesized DS NPs were investigated using transmission electron microscopy (TEM). The findings revealed marked enhancements in the properties relative to unreinforced PMMA. Compressive strength and Shore D hardness increasing by 21.88% and 9.16%, respectively. In addition, the W_r and COF were reduced by 33.76% and 29.88%. SEM observations confirmed that the incorporation of nanoparticles effectively minimized abrasive wear and surface cracking. Among all tested compositions, the 1.0 wt.% filler loading for both nanofiller exhibited the most exceptional performance characteristics.

Keywords: heat-polymerized PMMA, hydroxyapatite nanoparticles, date seed nanoparticles, compressive strength, Shore D hardness, wear rate, coefficient of friction.

INTRODUCTION

In recent years, researchers, academics, and industries have increasingly focused on polymer nanocomposites for their diverse applications in aerospace, automotive, electronics, military, and infrastructure sectors. The mechanical and tribological performance of these materials is critical due to their effectiveness as alternatives to metals, owing to their superior optical, mechanical, and electrical properties [1]. The introduction of clinical polymer nanocomposites resins revolutionized denture fabrication [2]. Within biomedical engineering, a variety of materials are employed for restorative components, bio-implants, bone cement fixation, prostheses, and dental dentures, with PMMA being one of the most widely utilized denture base material. Heat-polymerized PMMA is a clinically proven material that continues to serve as the gold standard for fabricating denture bases due to its extensive history of successful application [3]. PMMA powder typically contains PMMA, benzoyl peroxide as an initiator, plasticizers such as dibutyl phthalate, opacifiers like

titanium and zinc oxides, along with fibers and pigments or dyes. The liquid phase consists of methyl methacrylate (MMA) monomer, ethylene glycol dimethacrylate as a cross-linking agent, and hydroquinone as an inhibitor [4]. PMMA has long been considered the material of choice for denture base fabrication due to its biocompatibility, ease of processing, aesthetic qualities, and cost-effectiveness [5, 6]. However, despite its widespread application, PMMA has inherent limitations. Its relatively low mechanical properties make it prone to fracture during clinical use, with nearly two-thirds of dentures fracturing within the first three years, often at the midline or tooth–denture junctions [7]. These shortcomings highlight the need for further material enhancements [8, 9].

Recent studies have reinforced PMMA with fibers, metal oxides, polymers, and particularly nanofillers [10], which significantly enhance its mechanical properties such as flexural strength, hardness, and wear resistance as well as provide added functionalities like antimicrobial activity [11,12]. Aldwimi et al. [13] incorporated halloysite nanotubes (HNTs) with multi-walled carbon nanotubes (MWCNTs) into PMMA denture base composites and reported substantial enhancements in flexural strength (109.1 MPa) and tensile strength (64.4 MPa), along with moderate improvements in Vickers hardness. Similarly, Gad et al. [14] reinforced PMMA with zirconia nanoparticles and glass fibers, achieving superior flexural and impact strengths. The optimal formulation was identified as 2.5 wt.% ZrO_2 combined with 2.5 wt.% glass fibers, which delivered the best overall mechanical performance. Nabhan et al. [15] investigated a hybrid filler system of Al_2O_3/TiO_2 nanoparticles in PMMA denture bases. Their results showed that a filler content of 0.8 wt.% provided the most favorable improvements, reducing the coefficient of friction by up to 20% and the wear rate by 28% compared to unfilled PMMA. The systematic optimization of PMMA dental composite properties was achieved by Sinossi et al. [16] through the application of the Taguchi method, identifying that graphene filler incorporation of a 0.5 wt.% loading with heat-curing PMMA are the optimal parameters for minimizing COF and weight loss (WL) while maximizing hardness.

Alzayyat et al. [17] highlighted that low concentrations of SiO_2 nanoparticles were most effective in enhancing the flexural strength and elastic modulus of PMMA. In another study, Alrahlah et al. [18] examined PMMA reinforced with TiO_2 nanoparticles and found improvements in its mechanical properties, creep-recovery, and relaxation behavior. Kanie et al. [19] identified filler incorporation as one of the most effective strategies for enhancing the mechanical performance of composites. Zebarjad et al. [20] reinforced PMMA with high loadings of nano-hydroxyapatite (2.5–10 wt.%), which reduced ultimate and yield compressive strength but improved wear resistance. Aldabib [21] demonstrated that optimizing the concentration of a silane coupling agent significantly enhanced the tensile strength, flexural strength, and fracture toughness of HA-reinforced PMMA, as surface modification with γ-M silane improved interfacial bonding between PMMA and HA. In a related study, Aldabib and Ishak [22] showed that moderate HA filler levels enhanced flexural strength, modulus, and impact resistance, whereas excessive loading caused agglomeration and diminished performance. Similarly, Moudhaffar [23] reported that incorporating nano-ZrO_2 into PMMA led to marked improvements in mechanical properties.

The increasing focus on polymer composites reinforced with natural fibers and fillers stems from the global push for sustainability, the need to lower carbon emissions, and the pursuit of high-performance materials for advanced engineering application. Natural fiber and filler reinforced polymer composites demonstrate significant potential in sectors such as automotive, aerospace, biomedical prosthetics, sports equipment, and ballistic protection, where lightweight properties and high strength are essential [24, 25]. The efficient use of natural resources and waste materials is critical for promoting cleaner production and fostering sustainable development. Consequently, replacing synthetic fillers with natural alternatives in polymer composites has gained substantial interest, aligning with goals to reduce global carbon emissions. Industries like construction and automotive are increasingly investing in these eco-friendly composites due to their environmental, economic, and social advantages [26]. For instance, Xu et al. [27] reported that incorporating 1.5 mm chopped ramie fibers at 10 vol% loading increased the flexural modulus of heat-cured PMMA from 2.50 GPa to 3.46 GPa, though flexural strength declined at higher fiber contents, potentially due to inadequate interfacial bonding.

Similarly, Ruggiero et al. [28] observed improved adhesion, cohesion, and wear resistance in epoxy composites reinforced with waste date seed particles. A study by Saba et al. [29] demonstrated that a 50% loading of date palm fiber (DPF) in epoxy composites enhanced tensile strength, impact resistance, and morphological properties. In another study, Salih et al. [30] developed PMMA-based biocomposites reinforced with nanoscale pomegranate peel powder and Ajwa date seed powder at concentrations ranging from 0.4 to 1.6 wt.%. Their findings indicated notable improvements in mechanical properties compared to unreinforced PMMA. Rajkumar et al. [31] fabricated PMMA with seashell nanopowder loadings of 2, 4, 6, 8, 12, 16, and 20 wt.%, alongside an unfilled control specimen. Tribological testing revealed a significant enhancement in wear resistance. The composite containing 12 wt.% seashell nanopowder exhibited the optimal performance, demonstrating the lowest frictional force. However, a decline in performance was observed at higher filler contents, with the 16 wt.% and 20 wt.% composites.

While existing literature confirms that nanofiller incorporation significantly enhances the properties of PMMA, comparative studies on the effects of organic versus inorganic nanoparticles on the mechanical and tribological performance of PMMA denture resins remain limited. To address this research gap, the present study aims to fabricate PMMA-based denture composites reinforced with HA NPs and DS NPs. The specific objective is to assess the impact of incorporating 0.2–1.0 wt.% of these fillers on critical performance characteristics, namely the elastic modulus, compressive strength, wear resistance, and coefficient of friction. A further objective is to leverage low-cost organic nanofillers, such as those derived from DS NPs, to create an economical denture base reinforced material.

EXPERIMENTAL WORK

Materials

The denture base composites investigated in this study comprised a PMMA matrix reinforced with HA NPs and DS NPs. The matrix material, a heat-cured PMMA (Acrostone Dental & Medical Supplies Co., Cairo, Egypt), possessed a density of 1.18 g/cm³. Its polymerization was initiated using methyl methacrylate (MMA) monomer, a transparent, colorless liquid with a density of 0.93 g/cm³. The HA NPs (Nano Tech Co. for Photoelectronics, Cairo, Egypt) consisted of white, rod-like nanoparicles with a density of 3.02 g/cm³ and average dimensions of 100 ± 5 nm in length and 20 ± 3 nm in diameter.

Preparation and characterization of DS NPs

Two-dimensional sheet-like morphology as shown in Figure 1. Due to their atomically thin structure and high surface area-to-volume ratio, 2D nanomaterials exhibit behaviors markedly different from their bulk forms [32]. Numerous comprehensive reviews have underscored their scientific and technological significance, highlighting their exceptional characteristics such as extremely high surface area, mechanical flexibility, and highly tunable electronic properties [33, 34]. These advantages make them far superior to spherical or bulk nanoparticles for advanced applications in energy storage and harvesting, biomedical systems, and environmental remediation [35, 36].

Sample preparation

Figure 2 presents a schematic overview illustrating the experimental methodology employed in this study. The process began with the preparation of a control sample consisting of unreinforced, heat-cured PMMA to serve as a baseline for comparison against the nanofiller reinforced specimens. The composite samples were fabricated by mixing the PMMA monomer liquid with PMMA powder at a standardized ratio of 1:2 for approximately 5 minutes. Subsequently, nanofiller was incorporated into the PMMA matrix at varying concentrations of 0.2, 0.4, 0.6, 0.8, and 1.0 wt.%. The mixture was stirred thoroughly to ensure a homogeneous dispersion of the nanofillers within the acrylic resin prior to polymerization. The resulting nanocomposite slurry was then poured into cylindrical molds (8 mm diameter × 30 mm height) and compressed at 15 bar at room temperature for 45 minutes to compact the material and minimize porosity. The polymerization cycle was initiated by submerging the sealed molds in boiling water for 40 minutes, followed by a gradual, controlled cooling phase to room temperature to mitigate internal stresses and prevent crack formation. Finally, the cured cylindrical samples were carefully

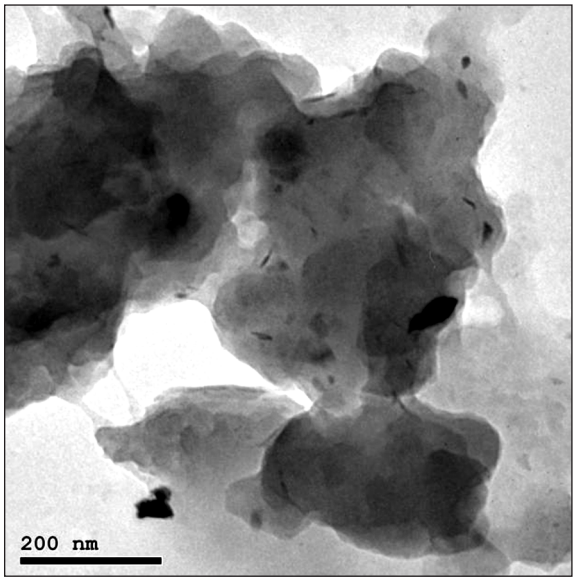

Figure 1. TEM image of prepared DS NPs

extracted and trimmed to the precise dimensions required for mechanical and tribological testing [37]. The prepared nanocomposite samples were systematically labeled based on their filler type and concentration. For the composites reinforced with HA NPs, the nomenclature was HA followed by a two-digit number indicating the weight percentage (e.g., HA02 for 0.2 wt.%, HA04 for 0.4 wt.%, HA06 for 0.6 wt.%, HA08 for 0.8 wt.%, and HA10 for 1.0 wt.%). Likewise, composites containing DS NPs were labeled DS02 for 0.2 wt.%, up to DS10 for 1.0 wt.% for the corresponding concentrations. The unreinforced PMMA control sample was distinctly labeled HD00.

Mechanical and tribological tests

For mechanical tests surface hardness was quantified using a Shore D durometer (ASTM D 2240) [38], which measures a material's resistance to indentation on a dimensionless 0–100 scale. The value is derived from the penetration depth (0–2.5 mm). For statistical reliability, five measurements were taken on both the top and bottom surfaces of each specimen, and the average value was reported. Compressive strength was determined according to ASTM D695 using a ZWICK Z010 universal testing machine.

Cylindrical samples were subjected to a uniaxial load at a crosshead speed of 1.3 mm/min until failure or until a maximum load of 10 kN was reached. For tribological tests gravimetric measurements of wear were obtained by determining the mass loss (Δm) for each sample pre- and post-experiment with a high precision analytical balance (±0.0001 g). Wear rate is a measure of how quickly a material wears down under specific rubbing or friction conditions, and

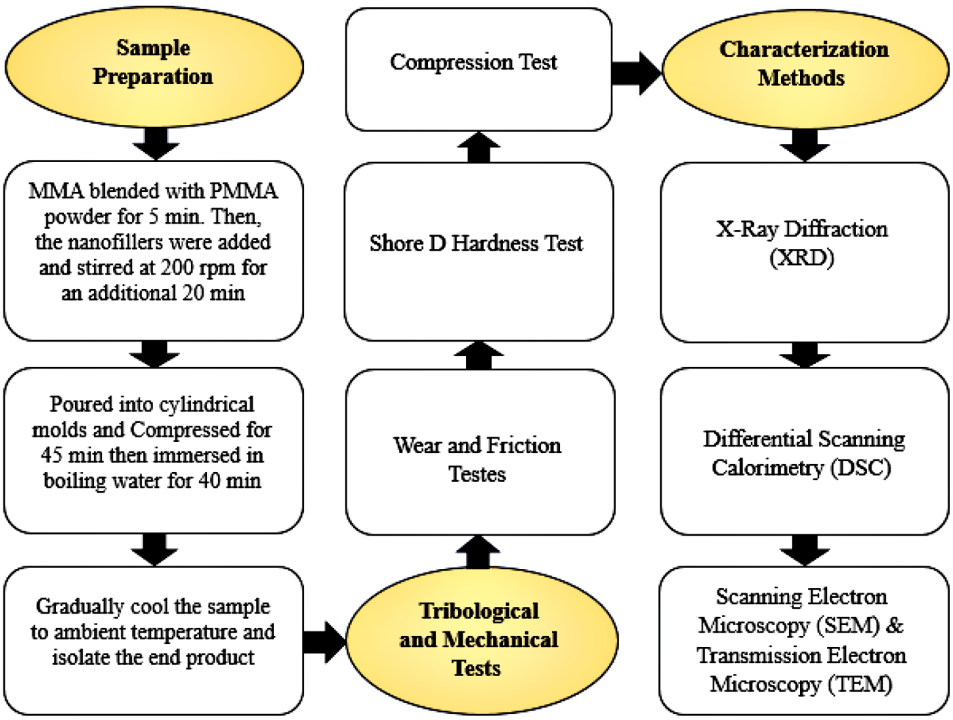

Figure 2. Flow chart summarizing the key experimental procedures

it is determined by a standard formula (Equation 1, 2). A pin-on-disc tribometer (Figure 3) was employed to simulate sliding wear under controlled conditions. The test material, configured as a stationary pin, was engaged against a rotating disc under incremental normal loads (4, 6, 8, 10, and 12 N).

Pin specimens were fabricated with a flat contact surface of 4 mm radius. All samples initially underwent turning processing to achieve surface smoothness, followed by precision lapping against 1000-grit SiC abrasive paper under controlled light load. This two-stage preparation protocol ensured uniform surface topography and perpendicular alignment to the sliding direction. The effectiveness of this methodology was validated through post-test examination of wear scar morphology, which consistently demonstrated complete and homogeneous contact across the entire pin surface.

To analyze performance across different interfacial scenarios, three distinct counterface materials were used: 1000-grit size emery paper, polished stainless steel, and PMMA. For emery paper to ensure reproducible abrasive wear conditions, a fresh 1000-grit SiC abrasive paper was used for each specimen, with a fixed test duration of 60 seconds. This approach minimized confounding effects from paper clogging or degradation, ensuring that measured wear responses solely reflected the material's resistance to a consistently sharp abrasive surface. All tests were conducted under controlled environmental conditions following ASTM G99-95 standards.

$$W_r = \frac{\Delta V}{F_N \cdot d} \tag{1}$$

$$\Delta V = \frac{\Delta m}{\rho}, d = 2\pi r \cdot N \tag{2}$$

The volumetric wear rate (W_r) is calculated by dividing the volume of material lost (ΔV) by the product of the applied normal force (F_N) and the total sliding distance (d). The volume loss (ΔV) is derived from the measured mass loss divided by the material density (ρ). For a pin-on-disk test configuration, the total sliding distance (d) is determined by the wear track radius (r) and the total number of revolutions (N) during the test.

For a pin-on-disk test configuration, the total sliding distance (d) is determined by the wear track radius (r) and the total number of revolutions (N) during the test. Pin-on-disc testing was performed against three distinct counterfaces to evaluate wear behavior under different contact conditions: (1) 1000-grit SiC abrasive paper with 14.5 µm particles (~2500 HV) adhesively bonded to the disc; (2) AISI 304 stainless steel with specified roughness parameters (Ra = 0.025 µm, Rz = 0.177 µm), 187 HV hardness, and 200 GPa modulus; and (3) cross-linked PMMA discs with Ra = 0.016 µm, Rz = 0.151 µm, 165 HV hardness, and 2.8 GPa modulus. This counterface selection enabled systematic investigation of abrasive, mixed adhesive-abrasive, and primarily adhesive wear mechanisms respectively, providing comprehensive assessment of the composite's tribological performance.

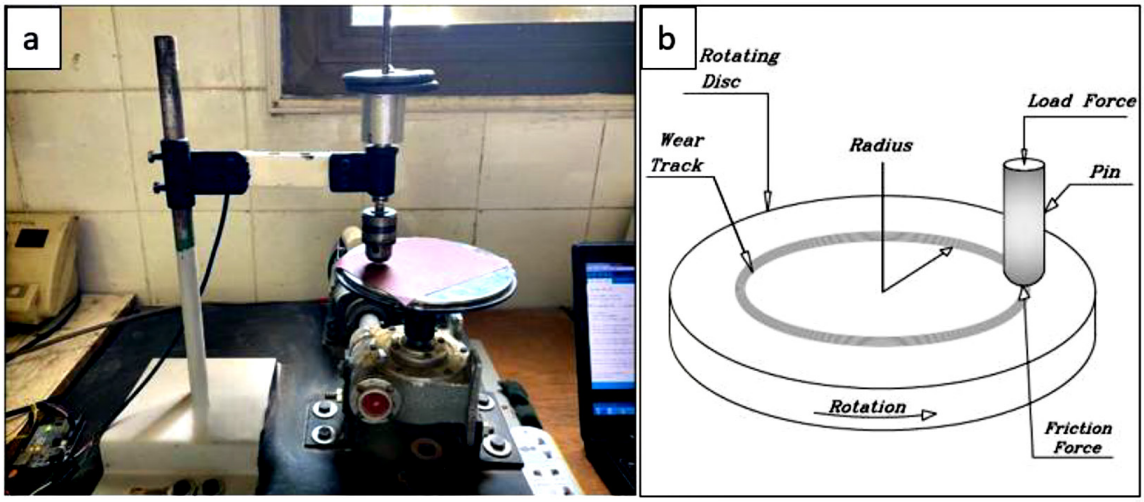

Figure 3. a) Pin-on-disc tribometer, b) representation of the pin-disc tribological contact

Thermal, structural, and microstructural analysis

X-ray diffraction (XRD) analysis was conducted using a Bruker D8 DISCOVER diffractometer (Bruker AXS GmbH, Germany) with a step size of 0.0205° (2θ) over a scanning range of 3–70°. The glass transition temperature (Tg) was determined by differential scanning calorimetry (DSC; Labsys DTA/DSC, Setaram, France). Samples of approximately 17.71 mg were heated at a rate of 10 °C/min. In addition, the surface morphology and wear characteristics of the composite specimens were analyzed using scanning electron microscopy (QUANTA FEG 250, FEI, USA). Furthermore, transmission electron microscopy (JEOL JEM-2100, JEOL, Japan) was used to investigate the morphology, dispersion, and crystallinity of the synthesized date seed nanoparticles (DS NPs).

RESULTS AND DISCUSSION

Figure 4 displays the average Shore D hardness results, evaluating the reinforcement efficacy of HA NPs and DS NPs and demonstrating the correlation between nanofiller concentration and the mechanical hardness of PMMA composites. The data indicate that HA NPs offering slightly better performance than DS NPs, whereas the unreinforced sample exhibited the lowest, demonstrated a baseline hardness of 85.42 (D index).

In comparison, the HA10 sample showed a 9.16% increase, reaching 93.25 (D index), while the DS10 composite exhibited an 8.65% improvement, attaining a hardness value of 92.81 (D index). These results confirm that nanoparticles significantly enhance surface hardness [39]. At higher filler loadings hardness decreased due to particle overcrowding, which created voids that served as crack initiation sites, promoting fracture through defect interconnection and particle matrix debonding [40, 41].

Figure 5 illustrates the compressive characteristics of PMMA nanocomposites, revealing a statistically enhancement in both compressive strength and elastic modulus upon the addition of nanofillers. Relative to the unreinforced polymer (HD00, 122.13 MPa), the compressive strength increased to 148.86 MPa for the HA10 composite and 143.81 MPa for DS10. A corresponding improvement was observed in the elastic modulus, which rose from 1.31 GPa (HD00) to 1.57 GPa (HA10) and 1.54 GPa (DS10). These findings confirm the effectiveness of HA NPs and DS NPs as reinforcing agents in strengthening the PMMA matrix, aligning with existing literature [42, 43].

The observed mechanical enhancement is primarily due to the role of nanofillers in bearing mechanical stress and restricting the mobility of polymer chains under load [13]. This reinforcement mechanism is directly influenced by the high modulus of the filler material, which enhances the composite's ability to resist deformation [44]. In addition, the size and distribution of particles play a critical role in determining the mechanical performance of composite materials [45]. However, at concentrations exceeding the optimal threshold, nanoparticle agglomeration induces structural defects that compromise mechanical performance a trend consistently documented in previous research [39, 46].

The tribological performance of the samples was assessed through abrasive wear tests against

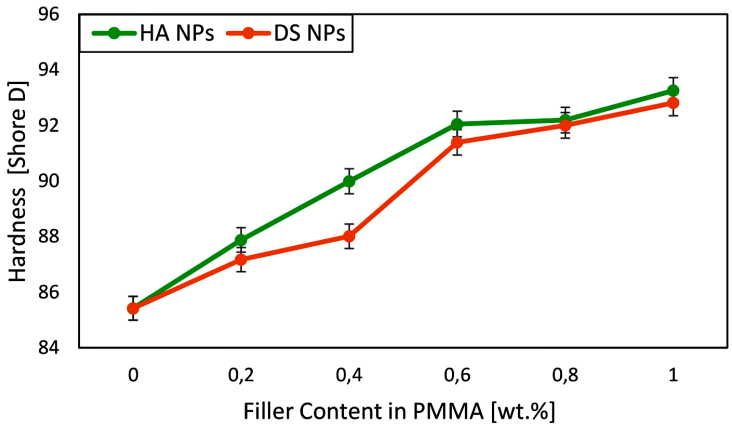

Figure 4. Hardness measurements vary systematically with the concentration of reinforcing nanofiller.

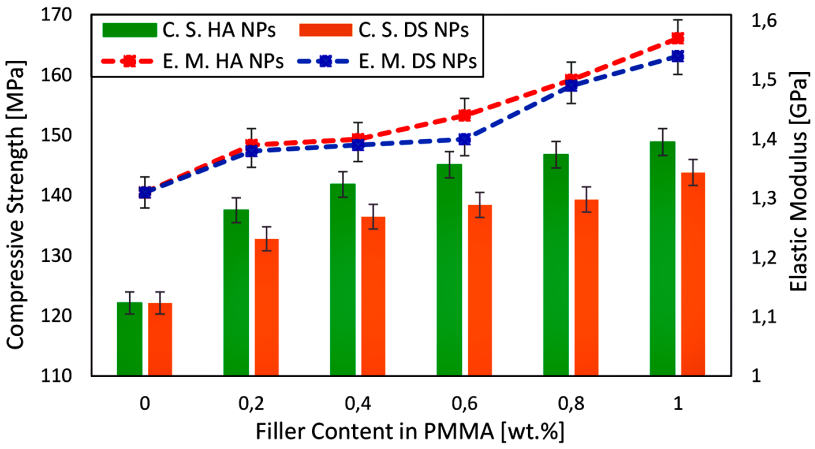

Figure 5. Compressive strength and elastic modulus for pure and nanocomposite polymers

1000-grit size emery paper under incremental normal loads (4–12 N). The use of relatively low loads in the wear tests was intentionally selected to mirror the actual functional conditions of denture base materials. In the oral environment, denture bases encounter only modest masticatory forces generally just a few newtons because the oral mucosa provides cushioning and the transmitted bite force through the denture is inherently limited. For this reason, a load range of 4–12 N was adopted to closely replicate the stresses generated during normal chewing and routine functional activities. This range ensures that the tribological assessment remains clinically meaningful, providing an accurate evaluation of the material's wear performance and structural reliability under realistic service loads, aligning with established methodologies in the field [15,47-49].

Gravimetric analysis revealed a consistent reduction in weight loss with increasing nanofiller HA NPs and DS NPs reinforcements, as illustrated in Figures 6, 7. Unreinforced PMMA exhibited the highest weight loss. Conversely, composites reinforced with either HA NPs or DS NPs demonstrated a progressive decline in wear, achieving minimal weight loss at the optimal loading of 1.0 wt.% with optimal tribological performance at 6 N for HA10 (Figure 6) and at 10 N for DS10 (Figure 7).

This enhancement is attributed to effective nanofiller dispersion and improved load bearing capacity within the polymer matrix [50]. Furthermore, weight losses increased proportionally with applied normal load for all nanocomposites, consistent with established tribological principles. Higher contact pressures induce greater shear stresses and frictional energy dissipation, thereby accelerating surface degradation [51, 52].

The relationship between nanoparticle concentration (HA NPs and DS NPs) and the COF in PMMA nanocomposites is demonstrated in Figures 8, 9. The optimal tribological performance was observed at a filler loading of 1.0 wt.%, where both the HA10 and DS10 composites exhibited an approximately 29% reduction in COF relative to unreinforced PMMA with maximum reduction at 6 N for HA10 (Figure 8) and at 4 N for DS10 (Figure 9), confirming the efficacy of nanofiller in enhancing surface lubrication. The reduction in COF varies significantly across composite systems and is influenced by the chemical properties, morphological features, and distribution of the filler within the polymer matrix [53]. Additionally, the results indicate that higher normal loads increase surface pressure and interfacial shear stresses resulting an elevated COF, this reinforces the conclusions drawn in earlier research [54].

The wear of unreinforced PMMA and the extreme wear values of the nanocomposites against emery paper were also compared against stainless steel and PMMA counterfaces. Figure 10 compares the weight loss and COF of the pure PMMA with nanocomposites containing 0.2 wt.% and 1.0 wt.% of HA NPs and DS NPs, tested against stainless steel and PMMA counterfaces. Evaluating the PMMA nanocomposites against emery paper, stainless steel, and PMMA does not merely quantify wear; rather, it provides a comprehensive assessment of their tribological behavior under diverse and demanding conditions. Such an approach enables a more authoritative conclusion regarding the material's performance and its suitability for practical applications. Tribological evaluation against a stainless steel counterface revealed that the HA10 and

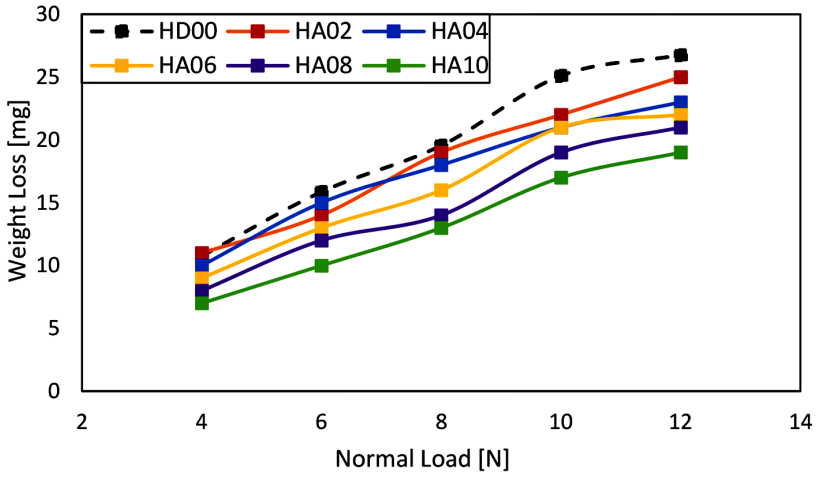

Figure 6. Weight loss for pure and nanocomposite polymers sliding against emery paper counterface HA NPs

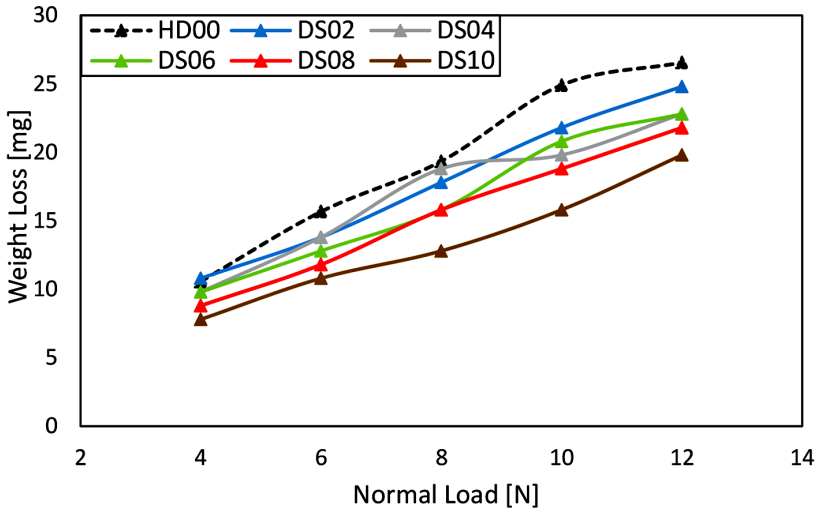

Figure 7. Weight loss for pure and nanocomposite polymers sliding against emery paper counterface DS NPs

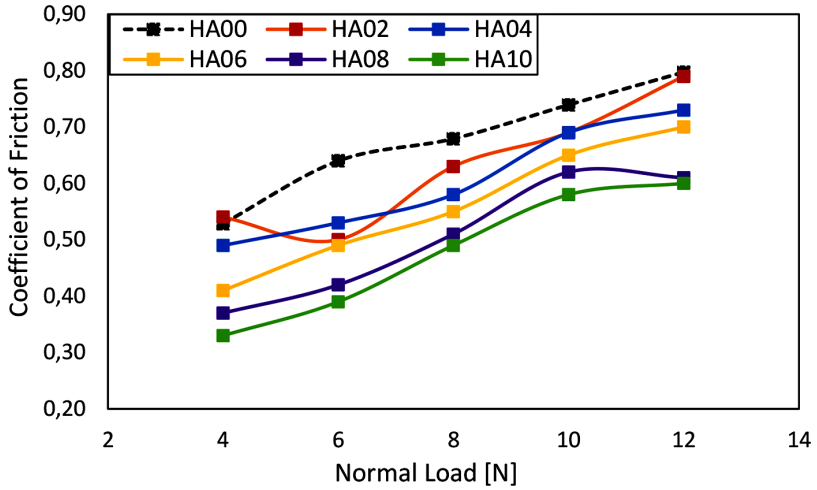

Figure 8. Coefficient of friction for pure and nanocomposite polymers sliding against emery paper counterface HA NPs

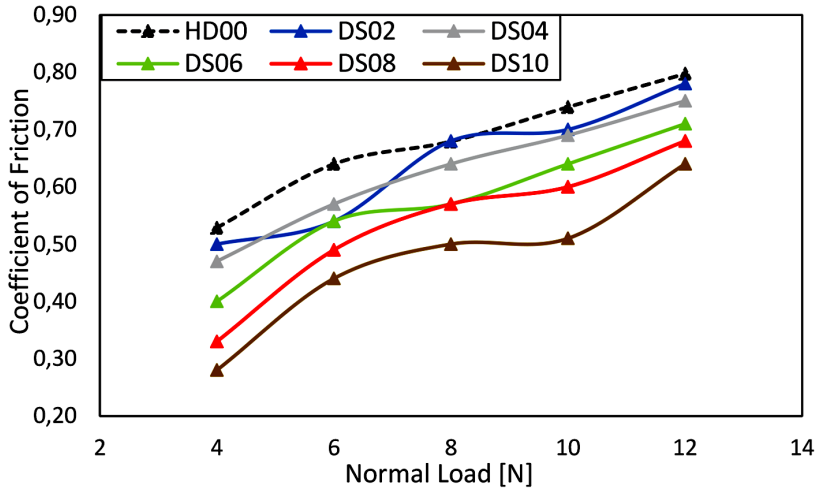

Figure 9. Coefficient of friction for pure and nanocomposite polymers sliding against emery paper counterface DS NPs

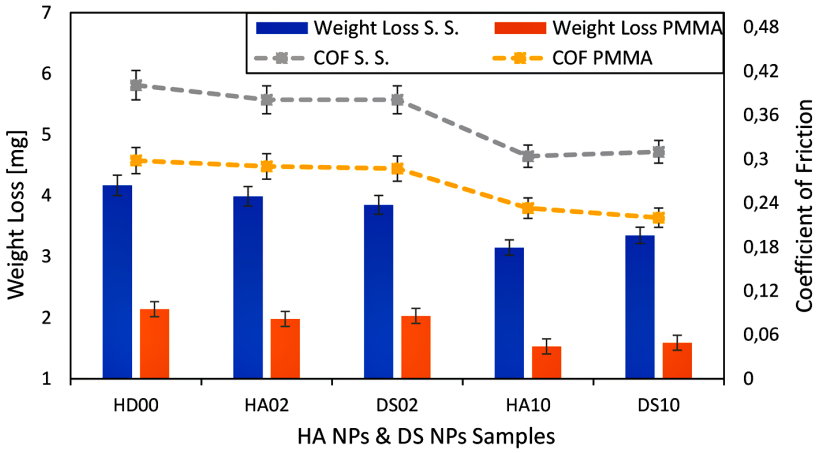

Figure 10. Weight loss and coefficient of friction for pure and nanocomposite polymers sliding against stainless steel and PMMA counterface

DS10 nanocomposites incurred reduced average weight losses of 3.15 and 3.35 mg, respectively, under a load range of 4–12 N.

This represents a marked improvement over the unreinforced PMMA, which exhibited a higher weight loss of 4.17 mg under identical testing conditions. When tested against a PMMA counterface, the nanocomposites maintained their superior performance. The HD00 sample displayed 2.14 mg weight loss, while the HA10 and DS10 composites achieved notably lower loss of 1.53 and 1.59 mg, respectively, confirming the enhanced wear resistance provided by both types of nanofiller across different interfacial conditions. Consistent with the wear results, the COF was reduced for the nanocomposites. Reductions of 24.18% (HA10) and 22.69% (DS10) were recorded against stainless steel, while against PMMA, the reductions were 21.81% (HA10) and 26.17% (DS10).

Figure 11 display the complete frictional behavior of the tested samples, including the optimal compositions (HA10 and DS10), the lower-performing formulations (HA02 and DS02), and the control sample (HD00), under an applied load of 4 N. The COF–time profiles clearly illustrate the distinct tribological responses among the formulations. The optimal samples (HA10 and DS10) exhibit a more stable and lower coefficient of friction throughout the test duration, indicating enhanced surface compatibility and effective load-bearing capability. In contrast, the lower-performing compositions (HA02 and DS02) and the control (HD00) show higher and more fluctuating

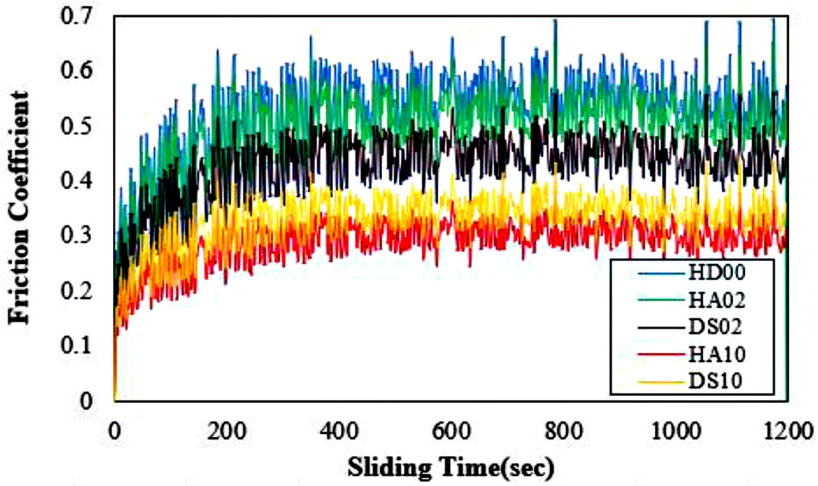

Figure 11. COF vs time for pure and nanocomposite polymers

COF values, reflecting increased surface interactions and less efficient frictional stability. These results confirm the beneficial influence of the optimized nanoparticle content on improving the overall frictional performance of the composite system.

Figure 12 presents the wear rates of the composite materials, categorized by counterface type. The results demonstrate that wear severity was directly influenced by the counterface, with emery paper causing the most substantial material loss, followed by stainless steel, and finally PMMA, which induced the least wear. Across all testing conditions, the unfilled control sample (HD00) consistently exhibited the highest wear rate, underscoring the enhanced wear resistance imparted by the nanoparticle fillers.

In contrast, the HA10 nanocomposite showed significantly enhanced wear resistance, reducing wear by 33.76%, 24.54%, and 28.76% on emery paper, stainless steel, and PMMA surfaces, respectively, compared to the unreinforced polymer. Similarly, the DS10 composite demonstrated considerable improvement, with wear reductions of 30.58%, 19.75%, and 25.96% on the corresponding counterfaces. A clear inverse correlation exists between hydroxyapatite and date seed nanoparticles concentration and the composite's wear rate. This behavior results from the incorporation of rigid ceramic particles (HA NPs), which enhance the material's surface hardness and thereby its resistance to abrasive wear [55]. The mechanical durability of pure PMMA is significantly enhanced through the strategic incorporation of optimal weight percentages of ceramic nanoscale reinforcements [56].

The tribological performance is further enhanced by the inherent lubricating properties of date seed nanoparticles, which perform as natural solid lubricants, consistent with findings in prior research [57].This functionality is achieved through two principal mechanisms: the generation of a protective tribofilm that shields the polymer from direct contact with the counterface, and the shear-induced reorientation of the nanoparticles' graphitic structures to form low-friction interfaces that promote smoother sliding.

Table 1 show the ANOVA results in Table reveal that both filler content and normal load have a statistically significant influence on the weight loss of the composite samples, as indicated by their very low P-values ($P = 0.000 < 0.05$). This confirms that variations in these factors meaningfully affect the wear behavior. The F-values further demonstrate that normal load ($F = 294.56$) has a much stronger effect than filler content ($F = 44.29$), indicating that the applied load plays a dominant role in determining the material's wear response. Overall, the analysis confirms that both parameters significantly affect the tribological performance, with normal load being the most influential factor in controlling weight loss during wear testing.

Figure 13 displays XRD patterns for HD00 sample and its nanocomposites HA02, DS02, HA10, and DS10. The pattern for the pure sample showed a primary broad peak at approximately 14.5° and two secondary low-intensity bands at 30.9° and 41.3°, consistent with previous studies [58,59]. Which indicating the non-crystalline nature of the PMMA polymeric structure [60].

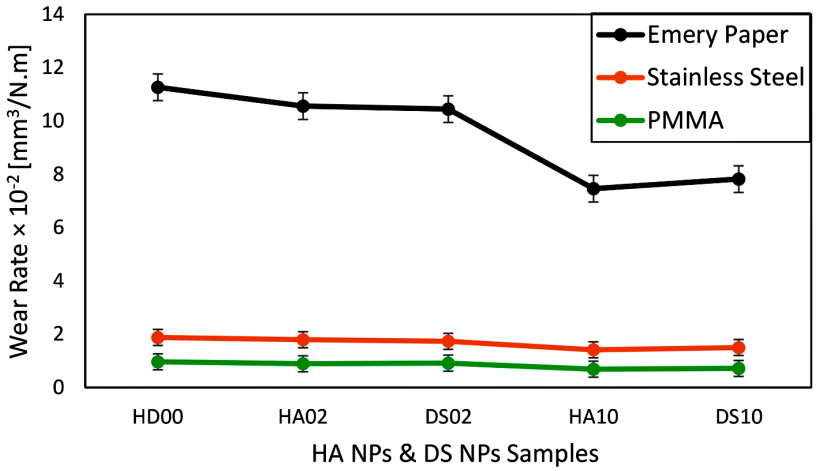

Figure 12. Influence of counterface material on wear rate for pure and nanocomposite polymers

Table 1. Analysis of variance for weight loss (mg)

Source	DF	SS	MS	F	P
Filler content	5	136.02	27.203	44.29	0.001
Normal load	4	723.64	180.911	294.56	0.001
Error	20	12.28	0.614		
Total	29	871.94			

Critically, all nanocomposite patterns retained this amorphous halo without exhibiting any new crystalline phases. This indicates that the incorporation of either HA NPs or DS NPs did not alter the amorphous nature of the PMMA matrix. The absence of additional peaks further confirms the lack of chemical interaction between the nanofillers and the polymer, suggesting that the reinforcement occurred primarily through physical dispersion without the formation of new chemical compounds or induced crystallization, this is congruent with prior findings [61, 62].

Differential scanning calorimetry (DSC) was performed on the control (HD00) and the top-performing composites, HA10 and DS10 (Figure 14). The glass transition temperature (Tg) increased from 84.76 °C for pure PMMA to 89.45 °C for DS10 and 97.83 °C for HA10. This significant rise in Tg indicates that both hydroxyapatite (HA) and date seed (DS) nanoparticles

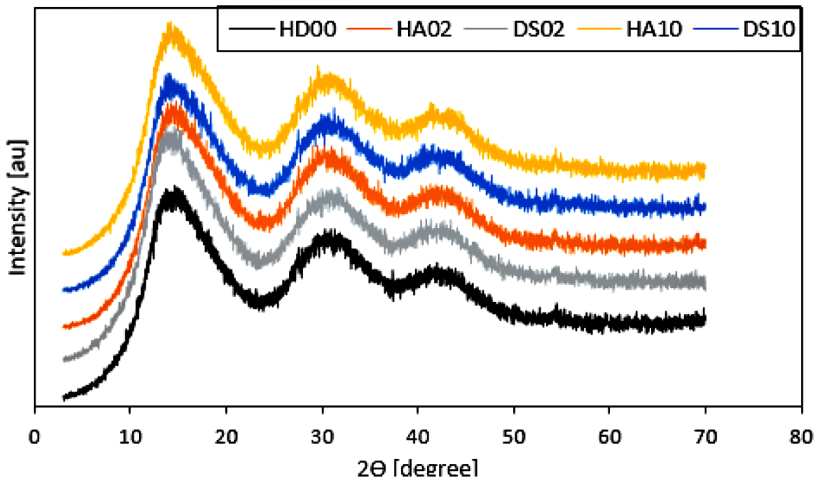

Figure 13. XRD pattern for pure and nanocomposite polymers

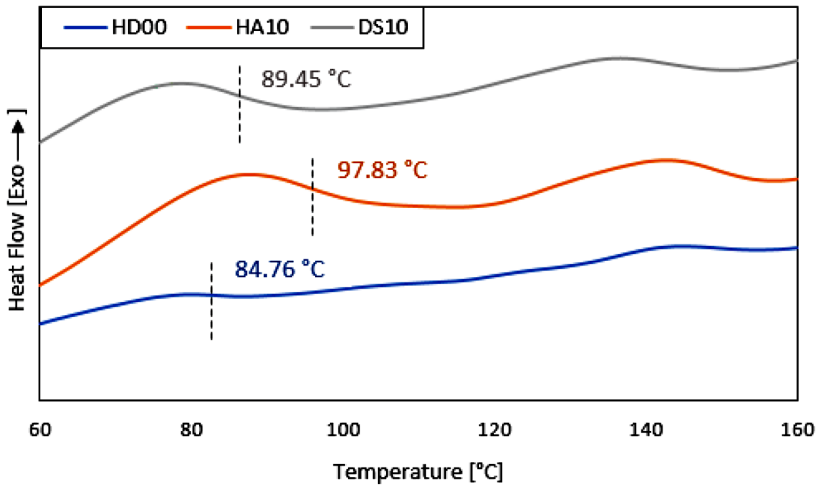

Figure 14. Differential scanning calorimetry curves for pure and nanocomposite polymers

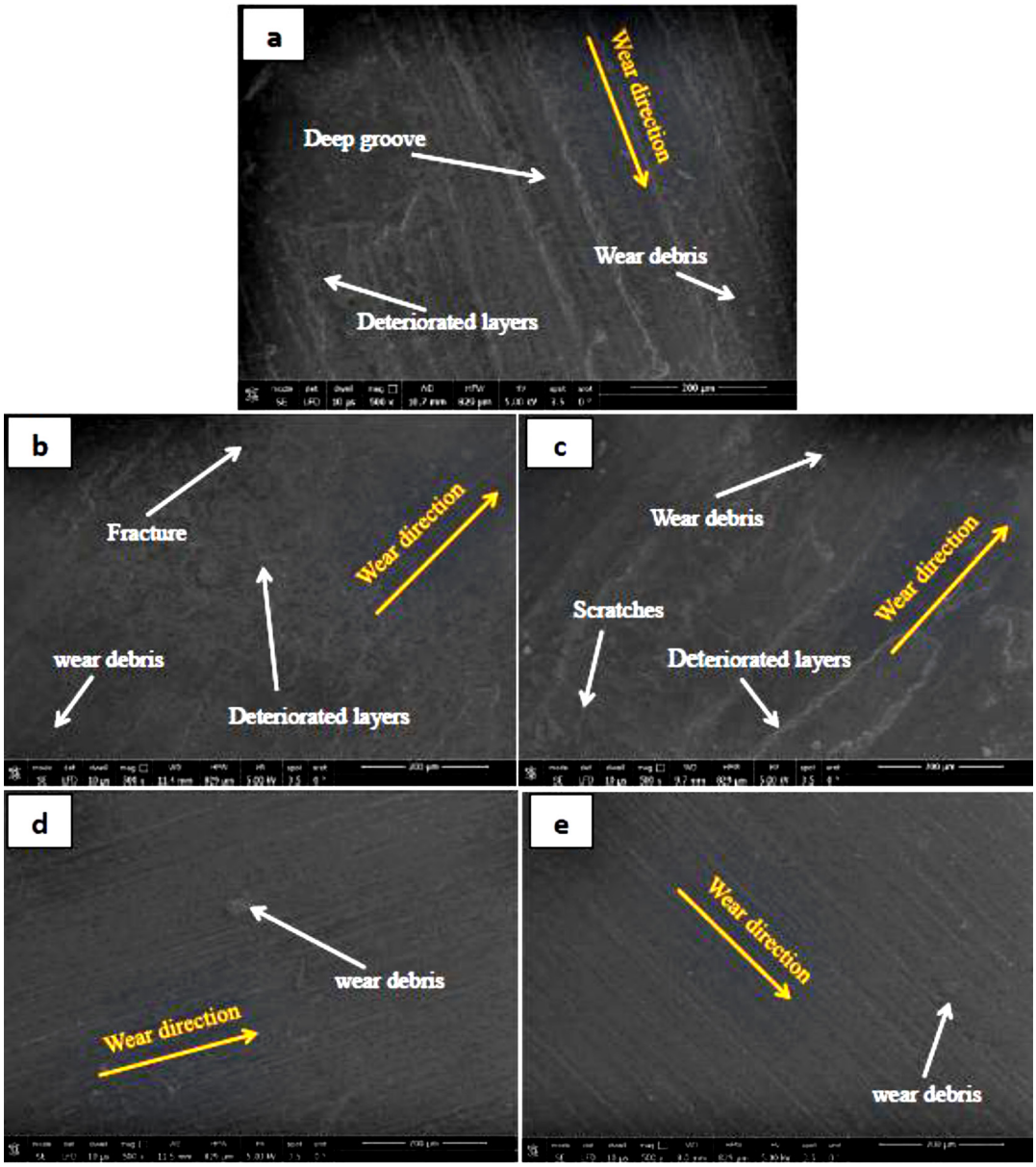

Figure 15. SEM micrographs of the worn surfaces for a) HD00, b) HA02, c) DS02, d) HA10, and e) DS10

enhance the thermal stability of the polymer, likely by promoting cross-linking and restricting chain mobility within the PMMA matrix [63, 64]

Figure 15 displays scanning electron microscopy images of the wear scars for samples HD00, HA02, DS02, HA10, and DS10. Figure 14a reveals severe surface degradation on the HD00 sample, manifested by deep abrasive grooves, delaminated layers, and adherent wear debris. These features collectively indicate pronounced adhesive and abrasive wear mechanisms arising from contact with a harder counterface. The observed grooving further confirms high interfacial shear stresses and intense contact during sliding, this finding aligns with previous studies [46]. At lower loading (0.2 wt.%), composites HA02 and DS02 (Figures 14b, c) also showed evidence of ploughing and cracking, with visible surface scratches, delaminated layers and debris formation. In contrast, composites with 1.0 wt.% nanofillers (HA10 and DS10, Figures 14d, e) exhibited notably smoother wear tracks with shallower scratches, a clear dependence on nanofiller concentration was observed. This improvement is attributed to enhanced stress transfer from the polymer matrix to the well-dispersed nanoparticles, which promotes more uniform load distribution, reduces localized stress concentrations, and effectively mitigates abrasive wear.

CONCLUSIONS

PMMA remains the primary material for denture bases owing to its history of use and practicality. Nevertheless, its limited mechanical strength often leads to fractures during function. In this study, the mechanical and tribological properties of reinforced nanocomposites were assessed for denture base applications. The formulation containing 1.0 wt.% HA nanoparticles delivered the most well-rounded enhancement, with a 21.88% increase in compressive strength, a 9.16% improvement in hardness, and a 29.29% and 33.76% reduction in the coefficient of friction and wear rate compared to pure PMMA. Similarly, the composite reinforced with 1.0 wt.% DS nanoparticles demonstrating a 17.75% increase in compressive strength, an 8.65% rise in hardness, and a 29.88% and 30.58% decrease in friction coefficient, along with wear rate.

Overall, the incorporation of nanoparticles significantly enhanced the wear resistance of PMMA across all tested counterfaces (emery paper, stainless steel, and PMMA), underscoring their effectiveness in improving the tribological reliability of denture base materials. Morphological analysis confirmed that the nanoparticles mitigated abrasive wear mechanisms by improving surface hardness and acting as solid lubricants. These findings confirm the potential of organic-inorganic nanofillers to develop advanced, durable dental materials with extended service life.

The main limitations of this work include the lack of direct interfacial temperature data and the restriction of time-dependent COF analysis to a single load. Consequently, future work will implement real-time thermal monitoring to quantify frictional heating and will extend the COF-versus-time measurements to higher loads for a more comprehensive tribological profile.

REFERENCES

1. Deleanu L, Botan M, Georgescu C. Tribological Behavior of Polymers and Polymer Composites. Tribology in Materials and Manufacturing - Wear, Friction and Lubrication. 2020. http://dx.doi.org/10.5772/intechopen.94264
2. Bilgin MS, Erdem A, Ağlarci OS, Dilber E. Fabricating Complete Dentures with CAD/CAM and RP Technologies. J Prosthodont. 2015;24 7:576–9. https://doi.org/10.1111/jopr.12302
3. Altalla H, Alawawda O, Bayindir F. Three-dimensionally printed versus conventional heat-polymerized PMMA denture base properties: A systematic review and meta-analysis. J Prosthet Dent. 2025. https://doi.org/10.1016/j.prosdent.2025.08.014
4. Alqutaibi AY, Baik AA, Almuzaini S, Farghal AEA, Alnazzawi AA, Borzangy S, et al. Polymeric denture base materials: a review. Polymers. 2023;15. https://doi.org/10.3390/polym15153258
5. Zafar MS. Prosthodontic applications of polymethyl methacrylate (PMMA): An update. Polymers. 2020;12. https://doi.org/10.3390/polym12102299
6. John J, Gangadhar SA, Shah I. Flexural strength of heat-polymerized polymethyl methacrylate denture resin reinforced with glass, aramid, or nylon fibers. J Prosthet Dent. 2001;86 4:424–7. https://doi.org/10.1067/mpr.2001.118564
7. Nejatian T, Johnson A, van Noort R. Reinforcement of denture base resin. Advances in Science and Technology. 2006;49:124–9. http://dx.doi.org/10.4028/www.scientific.net/AST.49.124
8. Meng T, Latta MA. Physical properties of four acrylic denture base resins. J Contemp Dent Pract.

2005;6 4:93–100. https://pubmed.ncbi.nlm.nih.gov/16299611/

9. Yadav P, Mittal R, Sood VK, Garg R. Effect of incorporation of silane-treated silver and aluminum microparticles on strength and thermal conductivity of PMMA. J Prosthodont. 2012;21 7:546–51. https://doi.org/10.1111/j.1532-849x.2012.00873.x
10. Majeed HF, Hamad TI, Bairam LR. Enhancing 3D-printed denture base resins: A review of material innovations. Sci Prog. 2024;107. https://doi.org/10.1177/00368504241263484
11. Gad MM, Fouda SM, Al-Harbi FA, Näpänkangas R, Raustia A. PMMA denture base material enhancement: a review of fiber, filler, and nanofiller addition. Int J Nanomedicine. 2017;12:3801–12. https://doi.org/10.2147/ijn.s130722
12. Stafford GD, Huggett R, MacGregor AR, Graham J. The use of nylon as a denture-base material. J Dent. 1986;14 1:18–22. https://doi.org/10.1016/0300-5712(86)90097-7
13. Aldwimi I, Alhareb A, Akil H, Hamid ZAA. Effect of hybrid nanofillers on the mechanical characteristics of polymethyl methacrylate denture base composite. Composite Materials. 2024. http://dx.doi.org/10.11648/j.cm.20240802.12
14. Gad MM, Al-Thobity AM, Rahoma A, Abualsaud R, Al-Harbi FA, Akhtar S. Reinforcement of PMMA denture base material with a mixture of ZrO_2 nanoparticles and glass fibers. Int J Dent. 2019;2019. https://doi.org/10.1155/2019/2489393
15. Nabhan AR, Taha M, Ghazaly NM. Filler loading effect of Al_2O_3/TiO_2 nanoparticles on physical and mechanical characteristics of dental base composite (PMMA). Polym Test. 2022. https://doi.org/10.1016/j.polymertesting.2022.107848
16. Sinossi MI, Abdu HM, Ameer AK, Hussein H. Optimization of graphene-based nanofiller combinations in pmma dental composites using Taguchi approach. Journal of the Egyptian Society of Tribology. 2025;22(3):80–97. https://doi.org/10.21608/jest.2025.398819.1125
17. Alzayyat ST, Almutiri GA, Aljandan JK, Algarzai RM, Khan SQ, Akhtar S, et al. Effects of SiO_2 incorporation on the flexural properties of a denture base resin: An in vitro study. Eur J Dent. 2021;16:188–94. https://doi.org/10.1055/s-0041-1732806
18. Alrahlah A, Fouad H, Fouad H, Hashem MA, Niazy AA, Al-Badah A. Titanium oxide (TiO_2)/polymethylmethacrylate (PMMA) denture base nanocomposites: mechanical, viscoelastic and antibacterial behavior. Materials. 2018;11. https://doi.org/10.3390/ma11071096
19. Kanie T, Fujii K, Arikawa H, Inoue K. Flexural properties and impact strength of denture base polymer reinforced with woven glass fibers. Dent Mater. 2000;16 2:150–8. https://doi.org/10.1016/S0109-5641(99)00097-4
20. Zebarjad SM, Sajjadi SA, Sdrabadi TE, Yaghmaei A, Naderi B. A study on mechanical properties of PMMA/hydroxyapatite nanocomposite. Engineering. 2011;3(8):795–801. http://dx.doi.org/10.4236/eng.2011.38096
21. Aldabıb JM. Effect of silane coupling agent content on mechanical properties of hydroxyapatite/poly (methyl methacrylate) denture base composite. Journal of Scientific Perspectives. 2021;5(1):37–45. https://doi.org/10.26900/jsp.5.1.04
22. Aldabib JM, Ishak ZAM. Effect of hydroxyapatite filler concentration on mechanical properties of poly (methyl methacrylate) denture base. SN Appl Sci. 2020;2(4):732. https://doi.org/10.1007/s42452-020-2546-1
23. MoudhaffarM, Ns I. Evaluation the effect of modified nano-fillers addition on some properties of heat cured acrylic denture base material. Journal of Baghdad college of dentistry. 2011;23:23–9.
24. Rashid A Al, Khalid MY, Imran R, Ali U, Koç M. Utilization of Banana Fiber-Reinforced Hybrid Composites in the Sports Industry. Materials. 2020;13. https://doi.org/10.3390/ma13143167
25. Malalli CS, Ramji BR. Mechanical characterization of natural fiber reinforced polymer composites and their application in Prosthesis: A review. Mater Today Proc. 2022. https://doi.org/10.1016/j.matpr.2022.04.276
26. Al-Oqla FM, Sapuan SM. Natural fiber reinforced polymer composites in industrial applications: feasibility of date palm fibers for sustainable automotive industry. J Clean Prod. 2014;66:347–54. https://doi.org/10.1016/j.jclepro.2013.10.050
27. Xu J, Li Y, Yu T, Cong L. Reinforcement of denture base resin with short vegetable fiber. Dent Mater. 2013;29 12:1273–9. https://doi.org/10.1016/j.dental.2013.09.013
28. Ruggiero A, Valášek P, Müller M. Exploitation of waste date seeds of *Phoenix dactylifera* in form of polymeric particle biocomposite: Investigation on adhesion, cohesion and wear. Compos B Eng. 2016;104:9–16. https://doi.org/10.1016/j.compositesb.2016.08.014
29. Saba N, Alothman OY, Almutairi Z, Jawaid M, Ghori W. Date palm reinforced epoxy composites: tensile, impact and morphological properties. Journal of Materials Research and Technology. 2019. https://doi.org/10.1016/j.jmrt.2019.07.004
30. Salih SI, Oleiwi JK, Mohamed A. Investigation of mechanical properties of PMMA composite reinforced with different types of natural powders. In 2018. https://doi.org/10.5281/zenodo.3837949
31. Rajkumar K, Sirisha P, Sankar MR. Tribomechanical and surface topographical investigations of poly

methyl methacrylate-seashell particle based biocomposite. Procedia materials science. 2014;5:1248–57. http://dx.doi.org/10.1016/j.mspro.2014.07.436

32. Hu J, Guo Z, Mcwilliams PE, Darges JE, Druffel DL, Moran AM, et al. Band gap engineering in a 2D material for solar-to-chemical energy conversion. Nano Lett. 2016;16 1:74–9. https://doi.org/10.1021/acs.nanolett.5b02895
33. Hu J, Guo Z, Mcwilliams PE, Darges JE, Druffel DL, Moran AM, et al. band gap engineering in a 2D material for solar-to-chemical energy conversion. Nano Lett . 2016;16 1:74–9. https://doi.org/10.1021/acs.nanolett.5b02895
34. Pomerantseva E, Gogotsi Y. Two-dimensional heterostructures for energy storage. Nat Energy. 2017;2. http://dx.doi.org/10.1038/nenergy.2017.89
35. Hasan MAM, Wang Y, Bowen CR, Yang Y. 2D nanomaterials for effective energy scavenging. Vol. 13, Nano-Micro Letters. Springer Science and Business Media B.V.; 2021. http://dx.doi.org/10.1007/s40820-021-00603-9
36. Bolotsky A, Butler D, Dong C, Gerace K, Glavin NR, Muratore C, et al. Two-dimensional materials in biosensing and healthcare: From in vitro diagnostics to optogenetics and beyond. ACS Nano. 2019 May 10;13(9):9781–810. https://doi.org/10.1021/acsnano.9b03632
37. Ameer AK, Mousa MO, Ali WY. Hardness and wear of polymethyl methacrylate filled with multiwalled carbon nanotubes as denture base materials. Journal of the Egyptian Society of Tribology. 2017;14(3):66–83. https://doi.org/10.21608/jest.2017.79494
38. Zhao HY, Allanson DR, Ren XH. Use of shore hardness tests for in-process properties estimation/monitoring of silicone rubbers. Journal of Materials Science and Chemical Engineering. 2015;03:142–7. http://dx.doi.org/10.4236/msce.2015.37019
39. Tjong SC. Novel nanoparticle-reinforced metal matrix composites with enhanced mechanical properties. Adv Eng Mater. 2007;9(8):639–52. https://doi.org/10.1002/adem.200700106
40. Ghazal M, Yang B, Ludwig K, Kern M. Two-body wear of resin and ceramic denture teeth in comparison to human enamel. Dent Mater. 2008;24 4:502–7. https://doi.org/10.1016/j.dental.2007.04.012
41. Shahdad S, Mccabe JF, Bull SJ, Rusby S, Wassell RW. Hardness measured with traditional Vickers and Martens hardness methods. Dent Mater. 2007;23 9:1079–85. https://doi.org/10.1016/j.dental.2006.10.001
42. Salih SI, Oleiwi JK, Hamad QA. Investigation of fatigue and compression strength for the PMMA reinforced by different system for denture applications. International Journal of Biomedical Materials Research. 2015;3(1):5–13. http://dx.doi.org/10.11648/j.ijbmr.20150301.13
43. Elkhouly HI, Ali EM, El-Sheikh MN, Hassan AESM. An investigated organic and inorganic reinforcement as an effective economical filler of poly (methyl methacrylate) nanocomposites. Sci Rep. 2022;12(1):16416. https://doi.org/10.1038/s41598-022-20393-3
44. Lee W, Hwang SG, Oh W, Kim CY, Lee JL, Yang EJ. Practical guidelines for hyaluronic acid soft-tissue filler use in facial rejuvenation. Dermatologic Surgery. 2019. https://doi.org/10.1097/dss.0000000000001858
45. Zebarjad SM, Sajjadi SA, Sdrabadi TE, Yaghmaei A, Naderi B. A study on mechanical properties of PMMA/hydroxyapatite nanocomposite. Engineering. 2011;3:795–801. http://dx.doi.org/10.4236/eng.2011.38096
46. Mackay ME, Tuteja A, Duxbury PM, Hawker CJ, Hawker CJ, Horn BA Van, et al. General strategies for nanoparticle dispersion. Science (1979). 2006;311:1740–3. https://doi.org/10.1126/science.1122225
47. Gallab M, Taha M, Rashed A, Nabhan A. Effect of low content of Al_2O_3 nanoparticles on the mechanical and tribological properties of polymethyl methacrylate as a denture base material. Egypt J Chem. 2022;65(8):1–9.
48. Taha M, Ibrahim AMM, AK A. Role of hybrid nanofiller GNPs/Al_2O_3 on enhancing the mechanical and tribological performance of HDPE composite. Sci Rep. 2023;13(1):1–13.
49. Fouly A, Nabhan A, Badran A. Mechanical and tribological characteristics of PMMA reinforced by natural materials. Egypt J Chem. 2022;65(4):543–53. https://doi.org/10.1038/s41598-023-39172-9
50. Ma J, Mo M, Du X, Dai S, Luck IJ. Study of epoxy toughened by in situ formed rubber nanoparticles. J Appl Polym Sci. 2008;110:304–12. https://doi.org/10.1002/app.27882
51. Basavarajappa S, Arun K V, Davim JP. Effect of filler materials on dry sliding wear behavior of polymer matrix composites - A Taguchi approach. Journal of Minerals and Materials Characterization and Engineering. 2009;08:379–91. http://dx.doi.org/10.4236/jmmce.2009.85034
52. Nuruzzaman DM, Chowdhury MA. Friction and wear of polymer and composites. 2012(6):231–245. https://doi.org/10.1504/IJSURFSE.2012.049056
53. Kato H, Komai K. Tribofilm formation and mild wear by tribo-sintering of nanometer-sized oxide particles on rubbing steel surfaces. Wear. 2007;262:36–41. http://dx.doi.org/10.1016/j.wear.2006.03.046
54. Keshavamurthy R, Tambrallimath V, Rajhi AA, M SAR, Patil AY, Khan TMY, et al. Influence of solid lubricant addition on friction and wear response of

3D printed polymer composites. Polymers. 2021;13. https://doi.org/10.3390/polym13172905

55. Dasari A, Yu ZZ, Mai YW. Fundamental aspects and recent progress on wear/scratch damage in polymer nanocomposites. Materials Science & Engineering R-reports. 2009;63:31–80. http://dx.doi.org/10.1016/j.mser.2008.10.001
56. Patel DK, Kumar S, Nandan G, Kumar SR. Assessment of physical and mechanical and tribological characteristics of poly methyl methacrylate denture based composites doped with nano ceramic particles: a review. International Journal of Polymer Analysis and Characterization. 2025; https://doi.org/10.1080/1023666X.2025.2504552
57. Ahmed MS, Nair KP, Tirth V, Elkhaleefa AM, Rehan M. Tribological evaluation of date seed oil and castor oil blends with halloysite nanotube additives as environment friendly bio-lubricants. Biomass Convers Biorefin. 2021; https://link.springer.com/article/10.1007%2Fs13399-021-02020-9
58. Motaung TE, Luyt AS, Bondioli F, Messori M, Saladino ML, Spinella A, et al. PMMA–titania nanocomposites: properties and thermal degradation behaviour. Polym Degrad Stab. 2012;97(8):1325–33. http://dx.doi.org/10.1016/j.polymdegradstab.2012.05.022
59. Yousefi F, Mousavi SB, Heris SZ, Naghash-Hamed S. UV-shielding properties of a cost-effective hybrid PMMA-based thin film coatings using TiO_2 and ZnO nanoparticles: a comprehensive evaluation. Sci Rep. 2023;13(1):7116. https://doi.org/10.1038/s41598-023-34120-z
60. Ahmad A, Rahman M, Su M, Hamzah H. Study of MG49-PMMA based solid polymer electrolyte. The Open Materials Science Journal. 2011; 5.
61. Bakr AM, Darwish AG, Azab AA, Awady ME El, Hamed AA, Elzwawy A. Structural, dielectric, and antimicrobial evaluation of PMMA/CeO_2 for optoelectronic devices. Sci Rep. 2024;14. https://doi.org/10.1038/s41598-024-52840-8
62. Saladino ML, Zanotto A, Martino DFC, Spinella A, Nasillo G, Caponetti E. Ce:YAG nanoparticles embedded in a PMMA matrix: preparation and characterization. Langmuir. 2010;26 16:13442–9. https://doi.org/10.1021/la9042809
63. Tian DJ, Chu X hui, Yu D, Yue Y, Zhao P, Sun XL, et al. Immobilization of polymethyl methacrylate brushes on hydroxyapatite under molecular weight control. Ind Eng Chem Res. 2011;50:6109–14. http://dx.doi.org/10.1021/ie102026p
64. Król-Morkisz K, Pielichowska K. Thermal decomposition of polymer nanocomposites with functionalized nanoparticles. Polymer Composites with Functionalized Nanoparticles. 2019. http://dx.doi.org/10.1016/B978-0-12-814064-2.00013-5